ANALELE UNIVERSITATII BUCUREŞTI

Department of Physical Chemistry
4-12 Regina Elisabeta Blvd, District 3, Bucharest
phone: +40-21-3143508; fax: +40-21-3159249
ISSN: 1844-0401

ARS DOCENDI PUBLISHING HOUSE
Sos. Panduri 90, District 5 Bucharest
phone/fax: +40-21-4102575
e-mail: arsdocendi@yahoo.com

DINITROGEN ACTIVATION BY DIRUTHENIUM COFACIAL DIPORPHYRIN COMPLEX. DFT STUDY

Natalya N. Gorinchoy *, **Iolanta I. Balan and I.Y. Ogurtsov**

abstract: Density functional theory and *ab initio* calculations are used to study the activation of dinitrogen by diruthenium cofacial diporphyrin complex [Ru_2DPB$(Im)_2$] (DPB= diporphyrinato-biphenylene tetraanion and Im= imidazole). The calculated equilibrium geometry of the formed complex [(μ-N_2)Ru_2DPB$(Im)_2$] was found to involve the flaring out of the diporphyrin's rings with a nearly linear dinitrogen bridge. The subsequent detailed analysis of the molecular orbitals (MOs) of this complex allows one to conclude that the dinitrogen activation is realized due to both the σ donation from the dinitrogen occupied bonding σ-MO to unoccupied *d*-AOs of the Ru atoms and the two-orbital back donation from two occupied MOs of the complex [Ru_2DPB$(Im)_2$] to the two splitting components of the unoccupied antibonding π*-MO of N_2.

key words: dinitrogen activation; *ab initio* calculations; DFT method; diruthenium complex

received: November 03, 2009 *accepted*: November 17, 2009

1. Introduction

The problem of dinitrogen activation by transition metal complexes is widely discussed in the literature (See, for example, reviews [1-3] and references therein). As a rule, among of the compounds containing moderately or strongly activated dinitrogen the dinuclear complexes prevail.

Iron is most utilized transition metal in biological dinitrogen fixation. Like iron, ruthenium is a catalyst component for some Haber-Bosch systems, and the dinitrogen complexes of ruthenium are often more stable than their iron congeners [3]. The discovery of a diruthenium cofacial diporphyrin complex [Ru_2DPB$(*Im)_2$] (where DPB= diporphyrinato-biphenylene tetraanion and *Im=1-*tert*-butyl-5-phenylimidazole) capable of binding dinitrogen to produce the [(μ-N_2)Ru_2DPB$(*Im)_2$] complex is an interesting example of ruthenium dinitrogen chemistry [4]. In [4] it is pointed out that the diruthenium cofacial diporphyrin Ru_2DPB, without the *Im molecules as the exterior ligands, does not react with dinitrogen, but Ru_2DPB$(*Im)_2$ does. It has been also established [5] that

* Laboratory of Quantum Chemistry, Institute of Chemistry, Academy of Science of Moldova, Academy str. 3, MD-2028 Chisinau, Republic of Moldova, *corresponding author e-mail:* ngorinchoy@yahoo.com

[(μ-N_2)Ru_2DPB(*Im)$_2$] is susceptible to protonation at the bridging dinitrogen. It means that the above compound must be at least *moderately activated* [2].

In [4] several possible binding geometries were proposed for the[Ru_2DPB(*Im)$_2N_2$] complex involving: a) doming of the porphyrin ligands, b) flaring out of the porphyrin rings, and c) bending of the Ru-N-N angles. However, to the best of our knowledge, thus far no experimental or theoretical data on the structure of this complex have been reported in the literature.

In the present work we calculate the equilibrium geometry of the [Ru_2DPB(Im)$_2N_2$] complex, evaluate the orbital charge transfers, and on this basis clarify which orbitals are responsible for dinitrogen binding and activation, explain the different behavior of the [Ru_2DPB] and the [Ru_2DPB(Im)$_2$] complexes with respect to dinitrogen addition.

To realize this plan the electronic structure calculations of three binuclear ruthenium complexes, Ru_2DPB (**I**), Ru_2DPB(Im$_2$) (**II**) and Ru_2DPB(Im)$_2N_2$ (**III**) , and also free N_2 and Im molecules were carried out in the frame of the density functional theory (DFT) and *ab initio* SCF-CI method.

2. Computational details

All calculations were performed using the PC GAMESS version [6] of the GAMESS (US) QC package [7]. For each compound considered, a full geometry optimization is performed by means of DFT calculations employing the B3LYP hybrid functional [8, 9]. All results were obtained from all-electron calculations; restricted (RHF) optimizations were carried out for singlet (low-spin) states, while all triplet (intermediate-spin) and quintet (high-spin) states were treated in the spin-unrestricted (UHF) framework.

Then, in order to clarify the spin states of the systems (**I-III**), SCF-CI energies were evaluated for the already optimized geometries (single point calculations only). The CI matrix included all configurations produced by single and double excitations from three highest occupied to the lower three unoccupied MOs, in the states with different appropriate values of the total spin S (S=0, 1, 2).

The size of the complexes makes it difficult the use of the extended basis sets. The following basis set was employed throughout the calculations: the Huzinaga's 3-21G [10] for the atoms of Ru, the 6-31G split valence basis set for the N atoms of dinitrogen [11], and the STO-6G [12] one for all other atoms.

To calculate the values of the orbital charge transfers to and from N_2, the MOs obtained by the DFT calculations are rewritten in the basis of the eigenfunctions of the free N_2 molecule and atomic orbitals (AO) of other atoms. Then the occupations of the N_2 eigenfunctions in the complex are calculated as the Mulliken populations of the corresponding orbitals.

3. Results and discussion

3.1 Structure of the Complexes

A general view of the complexes (**I**), (**II**), and (**III**) is shown in Fig.1. The geometry optimization was carried out in the assumption that the spatial nuclear configuration of all considered compounds corresponds to the C_{2v} point group of symmetry.

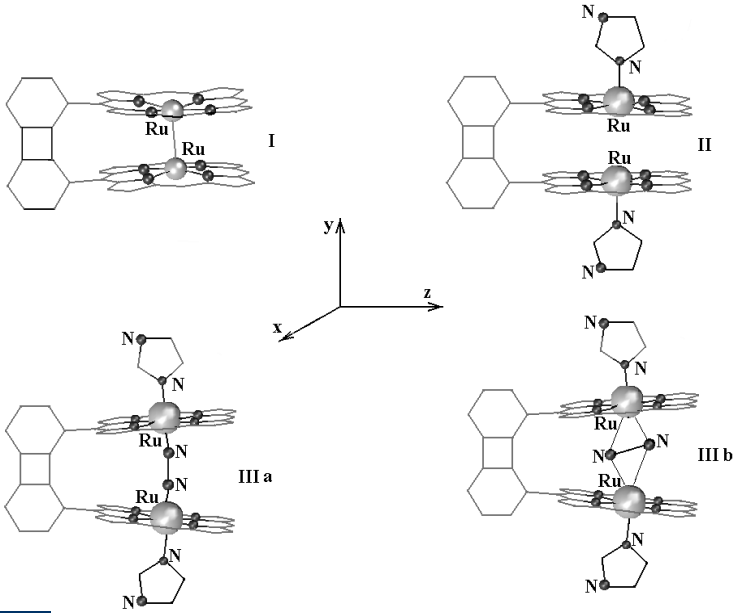

Fig. 1 *Structure of the [Ru_2DPB] (**I**), [Ru_2DPB(Im)$_2$] (**II**) and [Ru_2DPB(Im)$_2$ N_2] (**III**). (end-on **III a** and side-on **III b**) complexes* (for the sake of simplicity the hydrogen atoms are omitted).

The most relevant calculated geometry parameters for considered complexes are summarized in Table 1. The available experimental data for similar systems are given in parentheses. As can be seen, the method used in the present work provides structural parameters which are in close agreement with the experimental values [13,14].

Table 1 Calculated geometry parameters of (I)-(III) (bond lengths in Å and bond angles in degrees).

	[Ru_2DPB]	[Ru_2DPB(Im)$_2$]	[Ru_2DPB(Im)$_2N_2$]
Ru-N^{porph}	2.03 (2.05[13])	2.02	2.03
Ru-Im		1.92	1.98
Ru-Ru	2.45 (2.41[13])	3.80	
Ru-N			1.90 (1.94[14])
N-N			1.15 (1.12[14])
∠Ru-N-N			175.7 (177.9[14])

In the complex (**I**) each porphyrin skeleton has a domed conformation, the ruthenium atoms are displaced from the plane of the four coordinating nitrogen atoms (0.28Å for both Ru atoms) toward each other. A rather strong Ru-Ru bonding appears, the calculated values of

the Ru-Ru distance and the Ru-Ru bond order (*n*) are respectively *R*(Ru-Ru)=2.45Å, *n*(Ru-Ru)=1.02. This circumstance makes it difficult the dinitrogen insertion between the Ru atoms in this compound.

In the $[Ru_2DPB(Im)_2]$ (**II**) the electron density goes away from the Ru-Ru region to form the Ru-Im bonds that leads to the rupture of the Ru-Ru bond (*n*(Ru-Ru)≈0.). The Ru-Ru distance is quite large in this case (*R*(Ru-Ru)=3.80Å), the porphyrin rings are approximately parallel to each other, so that the dinitrogen addition to this compound becomes possible. Calculated energy gain of this process is large enough, ΔE=71.8 kcal/mol.

When searching for the equilibrium geometry of the $[Ru_2DPB(Im)_2N_2]$ complex, three different positions of the Im molecules with respect to the biphenylene plane were considered (Fig. 2): a) all three fragments are in the same plane , b) as in the first case, but the imidazol molecules are rotated with the angle of 180°, and c) the Im planes are perpendicular to the plane of biphenylene (the symmetry of the system in this case is C_2). Calculations show that the total energy of the system does not change significantly during rotation of the imidazol molecules with respect to the Ru-Ru line. The structure (**a**) in Fig.2 corresponds to the minimum of the total energy.

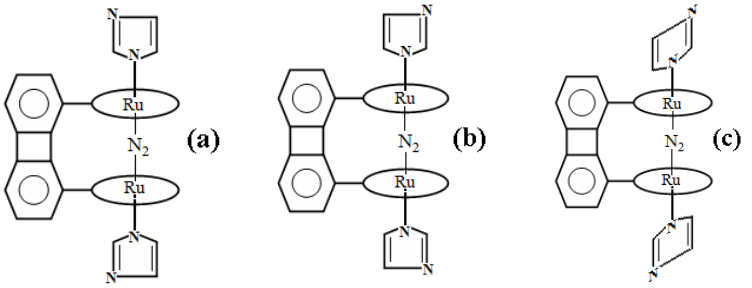

Fig. 2 *Three type of the Im coordination in (**III**).*

Two possible binding modes for bridged dinitrogen at the Ru-Ru cofactor (*end-on* bimetallic and *side-on* bimetallic) have been analyzed (**IIIa** and **IIIb** in Fig. 1). Calculations show that *end-on* binding of N_2 (**IIIa**) is preferred over *side-on* binding (**IIIb**) by 52kcal/mol.

Optimized equilibrium structure of the $[(\mu\text{-}N_2)Ru_2DPB(Im)_2]$ (**IIIa**) complex involves flaring out of the diporphyrin's rings, the angle between porphyrin planes being equal to 12.5°. The complex exhibits a slight bending of the Ru-N-N-Ru moiety with an Ru-N-N angle of 175.7°. The N-N bond length is elongated (by 0.04 Å) upon binding to the metal centers, compared to free N_2 (1.11 Å in our calculations and 1.098 Å - experimental value), N-N bond order decreases up to 2.63.

The value of the N-N stretching frequency (ν_{NN}) in the complex can be evaluated approximately using the harmonic oscillator equation, $\nu = 1/2\pi c\sqrt{K/\mu}$, where K is the N-N bond force constant, the reduced mass μ in our case is equal to the half of the mass of the N atom, and *c* is the velocity of light. The value of *K* was estimated in the assumption that the total energy *E* of the complex in the neighbourhood of the equilibrium N-N distance

can be written as $E(R_{NN}) = 1/2KR_{NN}^2$. Evaluated in this way the value of $\nu_{N\equiv N}$ is equal to 2130 cm^{-1}. For free dinitrogen we have obtained ν_{NN} =2310 cm^{-1} (experimental ν_{NN} =2331 cm^{-1} [3]). It is seen that the ν_{NN} is significantly reduced upon binding ($\Delta\nu_{NN}$ =180 cm^{-1}), indicating a weakening of the N-N bond.

3.2 Orbital charge transfers and the nature of the Ru-dinitrogen-Ru bonding

In analysing the electronic redistribution details in the [(μ-N_2)Ru_2DPB(Im)$_2$] complex it seems appropriate to use the definition of the ligand binding, in which mono-orbital, diorbital and multiorbital metal-ligand bonds are distinguished, suggested by Bersuker in the monograph [15]. In the MO terminology "the multiplicity of the orbital bonding (mono-, di-, and multiorbital) equals the number of complex-ligand bonding MOs uncompensated by the antibonding orbitals" [15]. It follows from this definition that the electron charge transfer to and from the ligand is due to formation of such uncompensated bonding molecular orbitals of the entire complex. The values of the orbital charge transfers depend on the nature of the metal and the geometry of ligand coordination. They may have opposite signs (Δq_i<0 means the electron density transfer from *i*-th MO of the ligand to the metal, and Δq_i>0 in the opposite case) compensating each other and giving a small value of the total charge transfer. However, their effect on ligand activation may be additive.

A molecular orbital energy-level scheme of the active valence zone of the whole [(μ-N_2)Ru_2DPB(Im)$_2$] complex and that of its fragments, [Ru_2DPB(Im)$_2$] and N_2, is given in Fig.3. Only those molecular orbitals which are involved in the Ru-N_2-Ru bonding are presented.

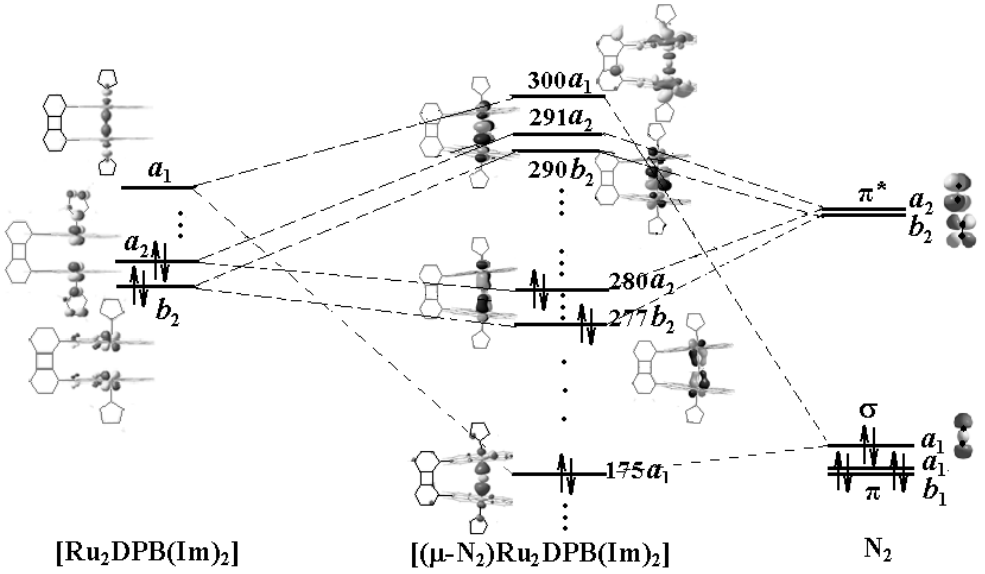

Fig. 3 *MO energy-level scheme for the bonding between N_2 and Ru_2DPB(Im)$_2$.*

Electronic structure calculations for each compound considered were carried out for three states with different appropriate values of the total spin S (S=0, 1, and 2). Both DFT and SCF-CI calculations show that the ground state of the complexes (**I**) and (**II**) is a singlet. For the $[(\mu\text{-}N_2)Ru_2DPB(Im)_2]$ the lowest triplet and singlet states were found to be sufficiently close in energy. The energy gap between them, $\Delta=E_{S=0}-E_{S=1}$, is approximately 5 kcal/mol in the DFT RHF(UHF) calculations and $\Delta \approx \pm 1$ kcal/mol in the SCF-CI calculations depending on the number of configurations taken into consideration. As it follows from the electronic structure analysis, the deep-lying one-electronic states responsible for the N_2 binding ($175\boldsymbol{a}_1$, $277\boldsymbol{b}_2$ and $280\boldsymbol{a}_2$ in Fig.3) are similar both in the singlet and triplet states. Therefore, further analysis and discussion of the electronic charge redistributions under the complex (**III**) formation are performed on the singlet states only.

It is to be noted that MOs of the $[Ru_2DPB(Im)_2]$ fragment on the left side of Fig. 3 are not pure *d*-AOs of the atoms of Ru (although contributions of them dominate in corresponding MOs), but contain some admixture of MOs of Im molecules and porphyrin rings.

In the coordinate system from Fig.1 the molecular orbitals of dinitrogen are transformed according to the following irreducible representations of the C_{2v} symmetry point group: HOMO of the σ-type belongs to a_1 representation, the double-degenerated π and π* MOs are splitting in the field of the complex into the two occupied (a_1 and b_1) and two unoccupied (a_2 and b_2) MOs (the right side in Fig.3). When forming the complex $[(\mu\text{-}N_2)Ru_2DPB(Im)_2]$, these valence MOs of the dinitrogen molecule interact with appropriate orbitals of the Ru atoms, giving rise to the Ru-N_2-Ru bonding.

One can see from Fig. 3, that three bonding MOs providing the Ru-N_2-Ru bonding are formed in the complex between the MOs of dinitrogen and the AOs of Ru atoms, each being uncompensated by antibonding orbitals (i.e. corresponding antibonding MOs are not occupied).

For ease of interpretation, we proceed in a more convenient local coordinate system, in which the z axis is directed along the Im-Ru-N_2-Ru-Im line. The orbital energies and the composition of these bonding and corresponding antibonding MOs are presented in Table2. The nomenclature of MOs in Table 2 is given in the above mentioned local coordinate system.

Table 2 One-electron states of valence zone of the $[(\mu\text{-}N_2)Ru_2DPB(Im)_2]$.

Orbitals	Energy, a.u.	Composition*
300 σ*	0.09	$0.57(4d_{z^2}^{Ru1}+4d_{z^2}^{Ru2})-0.35(\sigma^{NN})$
291 π_x*	0.02	$0.33(4d_{xz}^{Ru1}+4d_{xz}^{Ru2})- 0.67(\pi_x{}^{NN})$
290 π_y*	0.01	$0.32(4d_{yz}^{Ru1}+4d_{yz}^{Ru2})- 0.68(\pi_y{}^{NN})$
280 π_x	-0.14	$0.25\ (4d_{xz}^{Ru1}+4d_{xz}^{Ru2})+0.21(\pi_x{}^{NN})$
277 π_y	-0.16	$0.28(4d_{yz}^{Ru1}+4d_{yz}^{Ru2})+0.16(\pi_y{}^{NN})$
175 σ	-0.49	$0.21(4d_{z^2}^{Ru1}+4d_{z^2}^{Ru2})+0.32(\sigma^{NN})$

*For simplicity, only those contributions of the AOs of Ru and the MOs of N_2 are presented, whose coefficients are higher than 0.1 (in absolute value)

In Fig. 4 the fragments of three bonding MOs of the [(μ-N_2)Ru_2DPB$(Im)_2$] complex in the range of the Ru-N_2-Ru binding are presented along with the calculated values of the orbital charge transfers.

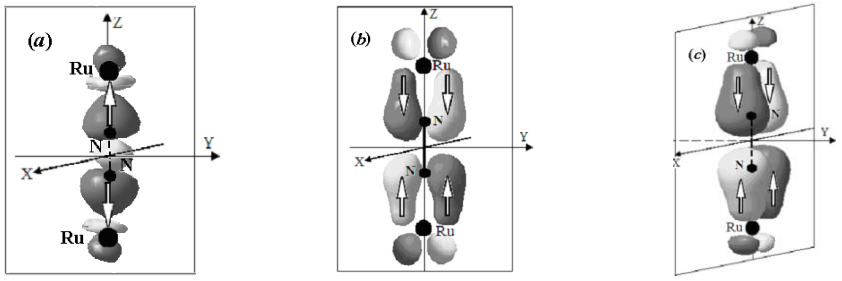

$\sigma \rightarrow d_{z2}$ $\Delta q(\sigma) = -0.19\bar{e}$ $d_{yz} \rightarrow \pi_y^*$ $\Delta q(\pi_y^*) = 0.30\bar{e}$ $d_{xz} \rightarrow \pi_x^*$ $\Delta q(\pi_x^*) = 0.38\bar{e}$

Fig. 4 *MO reprezentation of the $N_2 \rightarrow$ Ru donation and Ru$\rightarrow N_2$ back-donation.*

The occupied σ-MO of dinitrogen interacts with the unoccupied MO $\boldsymbol{a_1}$ of the [Ru_2DPB$(Im)_2$] fragment (the left side in Fig.3), which is mainly a symmetric linear combination of $4d_{z2}$ AOs of the Ru atoms, giving rise to the two σ-type MOs of the whole complex: the occupied bonding MO 175 **σ** and the unoccupied antibonding MO 300 **σ***. Due to the forming of the occupied 175 **σ** MO (Fig.4, ***a***) the electron density from the σ-MO of dinitrogen is transferred to the $4d_{z2}$-AOs of the Ru atoms (σ-type donation, Δq_σ). The results of the DFT calculations yield $\Delta q_\sigma = -0.19$ ē.

Two pairs of the π-type MOs of the [(μ-N_2)Ru_2DPB$(Im)_2$], 277$\boldsymbol{\pi_y}$ and 290$\boldsymbol{\pi_y}$*, 280$\boldsymbol{\pi_x}$ and 291$\boldsymbol{\pi_x}$, are formed from filled $\boldsymbol{a_2}$ (which is mainly a sum of $4d_{xz}$ AOs of the Ru atoms) and $\boldsymbol{b_2}$ (a sum of $4d_{yz}$ AOs of the Ru atoms) MOs of (**II**) and empty antibonding π_x*- and π_y*-MOs of dinitrogen. These two occupied π bonds provide the opposite charge transfer from ruthenium atoms to the antibonding π*-MO of N_2 (π-type back donation, Δq_π). Calculated values of the orbital charge transfers are quite significant, $\Delta q_{\pi x^*} = 0.38$ ē, $\Delta q_{\pi y^*} = 0.30$ ē (Fig.4, ***b***, ***c***). These values coincide with the decrease of the $4d_{xz}$ and $4d_{yz}$ AO populations of the Ru atoms due to formation of the complex.

Being of opposite signs, Δq_σ and Δq_π partially compensate each other, giving a smaller value of the total charge transfer (calculated resulting negative charge on dinitrogen is equal to -0.51ē). However, their effect on dinitrogen activation is additive.

Thus, all three molecular orbitals formed in the complex (**IIIa**) from MOs of dinitrogen and AOs of Ru atoms provide the dinitrogen binding and activation. Therefore the Ru-N_2-Ru bonding in the studied complex can be classified as mainly *three-orbital* one [15].

4. Conclusion

On the base of our DFT calculations the following conclusions can be drawn. Dinitrogen molecule in the [(μ-N_2)Ru_2DPB$(Im)_2$] complex is in its activated state. It is reflected in the corresponding elongation of the N-N bond distance accompanied by the decrease in the N-

N bond force constant and the stretching frequency $\nu_{N\equiv N}$. This activation is being realized both owing to donation of the σ-electronic density of dinitrogen to the atoms of Ru and back donation of rutheniums 4*d*-electronic density from two occupied molecular orbitals of the precursor complex [$Ru_2DPB(Im)_2$] to the unoccupied antibonding π* MO of the N_2 molecule.

REFERENCES

1. Fryzuk, M.D., Johnson, S.A. (2000) *Coord. Chem. Rev.* **200-202**, 379-409.
2. Studt, F., Tuczek, F. (2006) *J. Comput. Chem.* **27**, 1278-91.
3. MacKay, B.A., Fryzuk, M.D. (2004) *Chem. Rev.* **104**, 385-401.
4. Collman, J.P., Hutchison, J.E., Lopez, M.A. and.Guilard, R. (1992) *JACS* **114**, 8066-73.
5. Collman, J.P., Hutchison, J.E., Ennis, M.S., Lopez, M.A. and Guilard, R. (1992) *JACS* **114**, 8074-80.
6. Granovsky, Alex A. http://classic.chem.msu.su/gran/gamess/index.html.
7. Schmidt, M.W., Baldridge, K.K., eds. (1993) *J.Comput.Chem.* **14**, 1347-63.
8. Becke, A.D. (1993) *J. Phys. Chem.* **98**, 5648.
9. Lee, C., eds. (1988) *Phys. Rev*. **37**, 785.
10. Huzinaga, S., Andzelm, J., eds. (1984) **Gaussian Basis Sets for Molecular Calculations**, Elsevier, Amsterdam.
11. Ditchfield, R., Hehre, W.J., Pople, J.A. (1971) *J. Chem. Phys*. **54**, 724-728.
12. Hehre, W.J., Stewart, R.F., Pople, J.A. (1969) *J. Chem. Phys.* **51**, 2657.
13. Collman, J.P., Barnes, C.E., Swepston, P.N. and Ibers, J.A. (1984) *JACS* **106**, 3500-10.
14. Sellmann, D., Hille, A., Heinemann, F.W., Moll, M., Rosler, A., Sutter, J., Brehm, G., Reiher, M., Hess, B.A., Schneider, S, (2003) *Inorg. Chim. Acta* **348**, 194-8.
15. Bersuker, Isaac B. (1995) **Electronic structure and properties of transition metal compounds**, Chr. 6.3, John Wiley: New York, 213.